

IDENTIFYING PRIMORDIAL SUBSTRUCTURE IN NGC 2264

PAULA S. TEIXEIRA^{1,2}, CHARLES J. LADA¹, ERICK T. YOUNG³, MASSIMO MARENGO¹, AUGUST MUENCH¹, JAMES MUZEROLLE³, NICK SIEGLER³, GEORGE RIEKE³, LEE HARTMANN⁴, S. THOMAS MEGEATH¹, AND GIOVANNI FAZIO¹

ABSTRACT

We present new *Spitzer* Space Telescope observations of the young cluster NGC 2264. Observations at 24 μm with the Multiband Imaging Photometer has enabled us to identify the most highly embedded and youngest objects in NGC 2264. This letter reports on one particular region of NGC 2264 where bright 24 μm sources are spatially configured in curious linear structures with quasi-uniform separations. The majority of these sources ($\sim 60\%$) are found to be protostellar in nature with Class I spectral energy distributions. Comparison of their spatial distribution with sub-millimeter data from Wolf-Chase et al. (2003) and millimeter data from Peretto et al. (2005) shows a close correlation between the dust filaments and the linear spatial configurations of the protostars, indicating that star formation is occurring primarily within dense dusty filaments. Finally, the quasi-uniform separations of the protostars are found to be comparable in magnitude to the expected Jeans length suggesting thermal fragmentation of the dense filamentary material.

Subject headings: infrared: stars — open clusters and associations: individual (NGC 2264) — stars: formation — stars: pre-main-sequence

1. INTRODUCTION

NGC 2264 is an extended hierarchically structured young cluster (Lada & Lada 2003) associated with a giant molecular cloud in the Monoceros OB1 complex and located at a distance of 800 pc (e.g. Dahm & Simon 2005). The cluster is a very well studied region (e.g. Herbig 1954; Walker 1954), displaying evidence of ongoing star formation such as a plethora of molecular outflows (Margulis et al. 1988; Wolf-Chase et al. 2003) and Herbig-Haro objects (Reipurth et al. 2004). Luminous far infrared sources were detected by the Infrared Astronomical Satellite (IRAS), many of them being Class 0 and Class I sources (Margulis et al. 1989). However detailed study of the protostars in NGC 2264 was hampered by the limiting sensitivity and resolution of IRAS. The *Spitzer* Space Telescope provides significantly higher resolution and sensitivity. We have thus re-visited NGC 2264 by surveying the cluster with both the Infrared Array Camera (IRAC) and the Multiband Imaging Photometer for *Spitzer* (MIPS).

Here we present initial results of a MIPS and IRAC survey of a very young star forming region within NGC 2264, originally observed in the infrared by Sargent et al. (1984) and Schwartz et al. (1985). This particular region has been also observed at other wavelengths, namely in the sub-millimeter (Williams & Garland 2002; Wolf-Chase et al. 2003) and millimeter (Peretto et al. 2005). These observations reveal several filamen-

tary structures extending from a central IRAS source, IRAS 06382+0939 (also designated as IRAS 12 by Margulis et al. (1989) who classified it as a Class I source). IRAS 12's position appears to be a few arcseconds away from a near-infrared binary discovered by Castelaz & Grasdalen (1988), RNO-West (B-type star) and RNO-East (low-mass star). Simon & Dahm (2005) have photometric and spectroscopic observations of this binary in X-ray and near-infrared wavelengths and propose that RNO-E could be a proto-Herbig Ae star. Our *Spitzer* data indicate that IRAS 12 is in fact coincident with this binary. Several sub-millimeter cores (Williams & Garland 2002; Wolf-Chase et al. 2003) and millimeter cores (Peretto et al. 2005) are identified within these filaments. We compare results obtained with our *Spitzer* data with these sub-millimeter and millimeter observations in §3. Finally, we discuss primordial cluster sub-structuring in this region of NGC 2264 and compare these results with those found for the Trapezium (Lada et al. 2004) in §4.

2. OBSERVATIONS AND DATA REDUCTION

NGC 2264 was observed with IRAC as part of the *Spitzer* Guaranteed Time Observation program 37 (Fazio et al. 2004). The data were acquired in two epochs seven months apart (March 6, 2004 and October 8, 2004), with two dithers at each epoch to allow easy removal of asteroids and other transients. The total mosaicked area corresponds to $\sim 0.7^\circ \times 1.2^\circ$. The observations were performed in all IRAC bands (centered at 3.6, 4.5, 5.8 and 8.0 μm) using the 12 s IRAC High Dynamic Range mode, consisting of two consecutive exposures with 0.4 and 10.4 s integration time at each dither position. Basic data reduction and calibration were done with the *Spitzer* Science Center pipeline, version S10.5. A final mosaic was created for each of the two HDR exposures, using the SSC mosaic software the MOPEX (version 10/15/04), resampling the individual images on a final pixel scale of 0.86267"/pix ($1/\sqrt{2}$ of the original IRAC pixel scale) to have optimal point source registering at

¹ Harvard-Smithsonian Center for Astrophysics, 60 Garden Street, Cambridge, MA 02138, USA; pteixeira@cfa.harvard.edu, clada@cfa.harvard.edu, mmarengo@cfa.harvard.edu, gmuench@cfa.harvard.edu, tmegeath@cfa.harvard.edu, gfazio@cfa.harvard.edu.

² Departamento de Física da Faculdade de Ciências da Universidade de Lisboa, Portugal

³ Steward Observatory, University of Arizona, 933 North Cherry Avenue, Tucson, AZ 85721, USA; eyoung@as.arizona.edu, jamesm@as.arizona.edu, nsiegler@as.arizona.edu, griek@as.arizona.edu.

⁴ Dept. Astronomy, University of Michigan, 500 Church St., 830 Dennison Building, Ann Arbor, MI 48109, lhartm@umich.edu.

all IRAC bands. Cosmic rays and other outliers were removed using MOPEX temporal outlier module, and the diffuse background emission was matched between individual frames using the MOPEX overlap correction module.

We generated a list of point sources in each mosaic, at each wavelength, using the SExtractor package (Bertin & Arnouts 1996), and then performed aperture photometry using the IRAF routine APPHOT with an aperture radius of 2 pixels ($\sim 1.73''$). IRAC band merging was performed using the IDL function `srcor`⁵, where we used a matching radius of 2 pixels. The saturated sources had their magnitudes replaced with those obtained by the short exposure observations (0.4 s).

The MIPS (Rieke et al. 2004) observations were conducted on 2004 March 16 using the scan map mode. Fourteen scan legs of 0.75° length and $160''$ offsets were taken at medium speed. Total integration times of 80 s per point and 40 s per point were obtained in the $24\ \mu\text{m}$ band and $70\ \mu\text{m}$ band, respectively. We also obtained sparse coverage in the $160\ \mu\text{m}$ band, but most of those data were saturated due to the extremely high backgrounds from the molecular cloud. The full map was centered at $6^{\text{h}}40^{\text{m}}55^{\text{s}} +9^{\circ}37'08''$ with a position angle of 179° . These observations were processed with the MIPS Data Analysis Tool (DAT) (Gordon et al. 2005) which produces calibrated mosaics of the mapped regions. Processing of the resultant image products to obtain photometry was done using DAOPHOT and IDL routines. We used a zero point of 7.3 Jy for the $24\ \mu\text{m}$ magnitude scale.

3. RESULTS AND ANALYSIS

Figure 1 shows a color composite image of the region in NGC 2264 surrounding IRAS 12, which is the bright saturated source. The more extended nebulosity (green) in the image corresponds to polycyclic aromatic hydrocarbon (PAH) emission from the molecular cloud at $7.6\text{--}8\ \mu\text{m}$ and detected in the IRAC $8\ \mu\text{m}$ band. The brightest

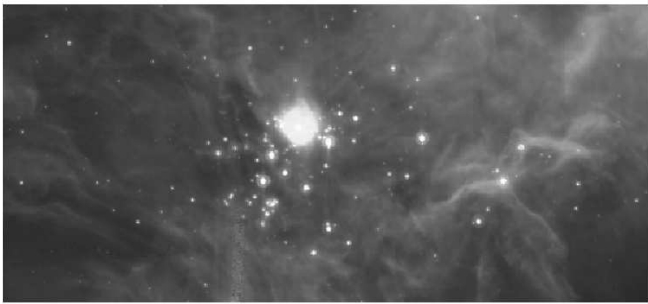


FIG. 1.— False color image of the Spokes cluster constructed from MIPS $24\ \mu\text{m}$ (red), IRAC $8.0\ \mu\text{m}$ (green), and IRAC $3.6\ \mu\text{m}$ (blue) data. The image shows unusual linear spatial alignments of the brightest $24\ \mu\text{m}$ sources. The central saturated source is IRAS 06382+0930 (IRAS 12).

$24\ \mu\text{m}$ sources (red) form several linear structures that are not clearly evident in the shorter wavelength data. The linear arrangements of the brightest $24\ \mu\text{m}$ sources appear as arms extending from the brightest source,

IRAS 12, resembling “spokes” of a wheel. We therefore refer to this region as the “Spokes” cluster. We performed two simple statistical tests to ascertain whether the linear spatial alignments of sources could occur by chance. The first test consisted of examining 10,000 synthetic fields, with randomly generated distributions of objects. Each field has the same number of objects as the bright $24\ \mu\text{m}$ sources in the Spokes cluster. These fields were searched for linear alignments that consist of 5 or more stars within a cone of an opening angle $< 10^\circ$ and a length $< 3'$. The second test consisted of radially binning the bright $24\ \mu\text{m}$ sources, using IRAS 12 as the center, and comparing the average bin density with a Poissonian distribution. Both tests yield a probability of 0.01-0.02% of finding an alignment of stars like that observed in the Spokes cluster.

To analyze the nature of the sources in the Spokes cluster we constructed Spectral Energy Distributions (SEDs) for all the sources in the selected field using *Spitzer* data. We determined the spectral indices, α_{IRAC} , of those sources detected in all four IRAC bands ($3.6\ \mu\text{m}$, $4.5\ \mu\text{m}$, $5.8\ \mu\text{m}$, and $8\ \mu\text{m}$) by performing a linear fit to the IRAC flux points in a $\log(\lambda)$ vs. $\log(\lambda F_\lambda)$ diagram, for each source. Identifying Class I objects as sources with $\alpha_{\text{IRAC}} > 0$ (Lada 1987), we estimate the total fraction of Class I $24\ \mu\text{m}$ sources in the entire field to be 33%. To better comprehend the spatial alignment of these

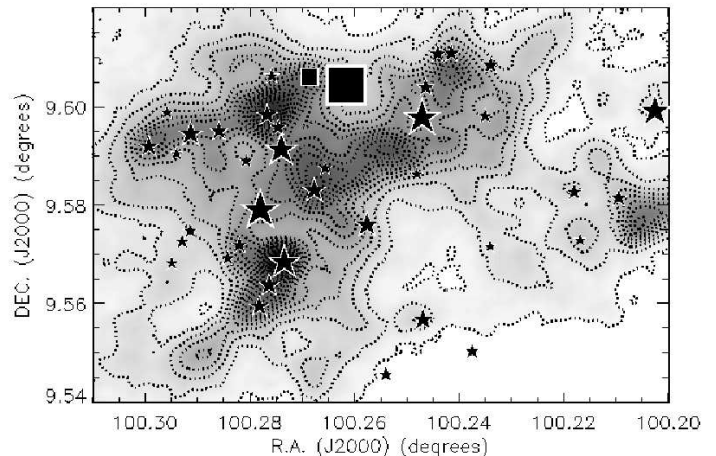


FIG. 2.— Comparison of the spatial locations of $24\ \mu\text{m}$ MIPS sources with dust emission at $850\ \mu\text{m}$ (SCUBA data courtesy from Wolf-Chase et al. (2003)). The greyscale and contours represent the sub-millimeter dust emission (contours range from 0 to 2 in steps of 0.1 Jy/beam), while the star symbols mark the position of the sources detected at $24\ \mu\text{m}$ with MIPS. The two squares mark the positions of the two brightest $24\ \mu\text{m}$ sources (< 2 magnitudes). The sizes of the star and box symbols are proportional to the magnitude of the sources (ranging from 2.0 to 6.0 magnitudes for the star symbols). The beam size for the $850\ \mu\text{m}$ data is indicated in the lower right corner.

protostars we examine sub-millimeter observations by Wolf-Chase et al. (2003) which trace dust emission from dense molecular gas. Figure 2 shows $850\ \mu\text{m}$ emission detected in the region (Wolf-Chase et al. 2003). The star

⁵ from IDL Astronomy User's Library: <http://idlastro.gsfc.nasa.gov/homepage.html>, adapted from software from the Ultraviolet Imaging Telescope.

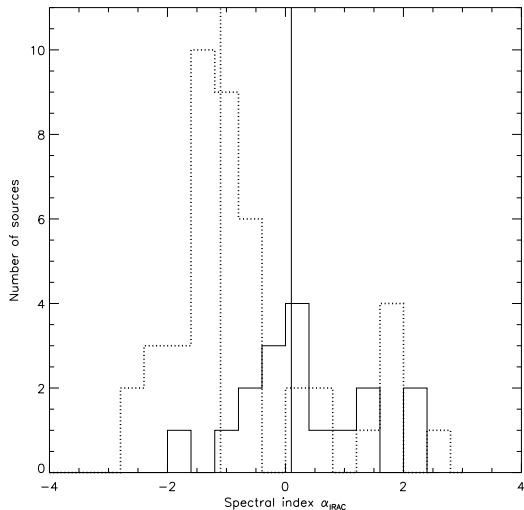


FIG. 3.— Diagram of the distribution of spectral indices for sources detected at $24\mu\text{m}$ within (solid line) the $850\mu\text{m}$ 0.4 Jy/beam contour (see Figure 2), and for the remaining sources in the field (dotted line). The vertical solid line corresponds to the median of the distribution of spectral indices of sources inside the contour, $\alpha_{\text{IRAC}}=0.1$, whereas the vertical dotted line corresponds to the median of the distribution of spectral indices of sources outside the contour, $\alpha_{\text{IRAC}}=-1.1$.

symbols mark the positions of the bright $24\mu\text{m}$ sources and the symbol sizes are proportional to the magnitudes of the sources. It is remarkable how well the bright $24\mu\text{m}$ sources are aligned with the dusty filaments. The same result is obtained when using the $450\mu\text{m}$ data, also from Wolf-Chase et al. (2003). The comparison with the sub-millimeter data shows that the linear alignments have drawn our eye to filaments of the interstellar medium that appear to be breaking up and forming stars in a very regular pattern.

We compare the distribution of α_{IRAC} for sources within the dusty filaments and for sources in the surrounding region, using the $850\mu\text{m}$ 0.4 Jy/beam contour in Figure 2 as the boundary separating these two regions. Figure 3 shows a histogram of the spectral indices determined for both the $24\mu\text{m}$ sources within (solid line) and outside (dotted line) this contour. The diagram in Figure 3 shows that there is a higher concentration of Class I sources within the dusty filaments, as seen by comparing the median values of α_{IRAC} for both distributions: 0.1 for sources inside the filaments and -1.1 for the remaining surrounding sources. The fraction of Class I $24\mu\text{m}$ sources within the dusty filaments is 59% whereas for outside the filaments it is 23%. Not all the $24\mu\text{m}$ sources in the Spokes cluster have detections in all the IRAC bands. Of these remaining sources that have at least 3 band (IRAC and MIPS) detections we find 7 with rising slopes. We list all the Class I sources that we identified within the dusty filaments in Table 1, sorted by their $24\mu\text{m}$ magnitude. The spectral index α_{IRAC} is tabulated in column 4. We note that there are two $24\mu\text{m}$ sources within the dusty filaments that have no IRAC counterpart, and as such we were not able to classify them. These sources could also be very young protostars.

Recent millimeter observations by Peretto et al. (2005) identify 1.2 mm emission peaks in this region that we find

are spatially coincident with 9-10 of the sources listed in Table 1⁶ (other millimeter sources detected outside the filaments also have IRAC and/or MIPS detections).

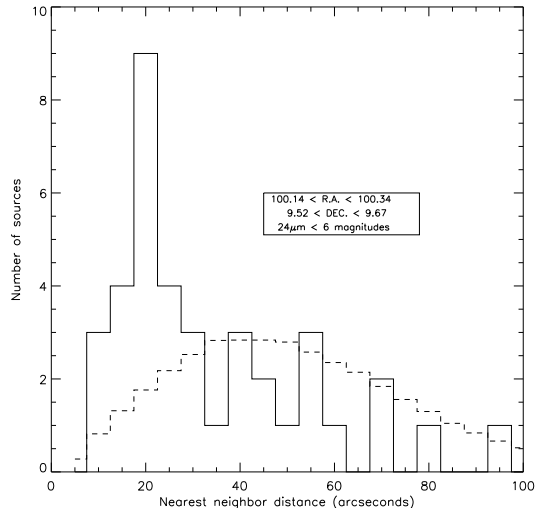


FIG. 4.— Histogram of the nearest neighbour distances between the $24\mu\text{m}$ sources in the Spokes cluster (solid line). We have restricted this sample to sources brighter than the 6th magnitude at $24\mu\text{m}$. The dashed line histogram corresponds to the averaged nearest neighbour distance distributions of 10,000 simulated fields populated with randomly positioned stars (see text for details). The preferential separation between the observed $24\mu\text{m}$ sources is $20'' \pm 5''$.

Finally, we analyse the spatial separations of the protostars in the Spokes cluster. Figure 4 shows a histogram (solid line) of the nearest (projected) neighbor separations between the brightest $24\mu\text{m}$ sources in the Spokes cluster. There is a clear peak in the distribution corresponding to a separation of $20''$. The mean separation of sources in this distribution is $26''$. By using Monte Carlo techniques, we generated 10,000 synthetic star fields of the same area and number of stars as in the observed field. The dashed-line histogram in Figure 4 corresponds to the averaged nearest neighbor distributions of these simulated fields. We calculated the probability of generating a field with the same fraction of sources, i.e. 44.7%, with nearest neighbor separations between $15''$ and $25''$ as in the Spokes cluster field. The probability of finding a field with a 40% or greater fraction of sources with those separations is 0.08%. The $20''$ peak is therefore very unlikely a random feature.

Williams & Garland (2002) determined a mean density from their sub-millimeter observations of $3 \times 10^4\text{ cm}^{-3}$ for the dense gas in the Spokes cluster. Assuming a temperature of 17 K (Ward-Thompson et al. 2000) the corresponding Jeans length for this density is 0.105 pc or $27''$ at a distance of 800 pc. For a mean density of $4.2 \times 10^4\text{ cm}^{-3}$ the corresponding Jeans length would be $20''$. These Jeans lengths agree very well with the separations we measure, possibly indicating that the dense filaments have thermally fragmented into quasi-equidistant cores where the stars are now forming. This

⁶ specifically D-MM1, D-MM2, D-MM3, D-MM6, D-MM8, D-MM9, D-MM10, D-MM13, and D-MM15 from Peretto et al. (2005), corresponding to sources with # 4, 9, 7, 16, 5, 10, 15, 11, and 2, respectively.

TABLE 1
CLASS I SOURCES IN THE SPOKES CLUSTER DUSTY
FILAMENTS

ID	position (J2000)		α_{IRAC}	$m_{[24\mu\text{m}]}$ (mag.)
	R.A.	DEC.		
1	06 ^h 41 ^m 02.8 ^s	+09°36'16"	...	0.44
2	06 ^h 41 ^m 04.5 ^s	+09°36'21"	2.33 ^a	1.00
3	06 ^h 41 ^m 05.8 ^s	+09°35'29"	0.52	2.20
4	06 ^h 41 ^m 05.6 ^s	+09°34'08"	0.03 ^b	2.21
5	06 ^h 41 ^m 01.8 ^s	+09°34'34"	0.13	2.93
6	06 ^h 41 ^m 09.9 ^s	+09°35'41"	2.36	2.94
7	06 ^h 41 ^m 04.3 ^s	+09°34'59"	0.09	3.07
8	06 ^h 41 ^m 06.3 ^s	+09°33'50"	1.36	3.33
9	06 ^h 41 ^m 06.5 ^s	+09°35'54"	3.26 ^b	3.42
10	06 ^h 41 ^m 06.8 ^s	+09°33'35"	1.42 ^c	3.54
11	06 ^h 41 ^m 08.6 ^s	+09°35'42"	1.99 ^b	3.87
12	06 ^h 40 ^m 58.0 ^s	+09°36'40"	1.15	4.11
13	06 ^h 40 ^m 59.1 ^s	+09°36'15"	0.65 ^b	4.11
14	06 ^h 40 ^m 58.6 ^s	+09°36'39"	1.23	4.19
15	06 ^h 41 ^m 07.7 ^s	+09°34'19"	2.22	4.29
16	06 ^h 40 ^m 58.0 ^s	+09°36'15"	0.12	6.77
17	06 ^h 41 ^m 04.5 ^s	+09°33'44"	0.02	7.22

^a α_{IRAC} determined by fitting 3.6 μm , 4.5 μm , and 8.0 μm

^b α_{IRAC} determined by fitting 4.5 μm , 5.8 μm , and 8.0 μm

^c α_{IRAC} determined by fitting 5.8 μm , 8.0 μm , and 24 μm

result is reminiscent of that found in the Taurus clouds by Hartmann (2002).

4. DISCUSSION AND CONCLUSIONS

Our analysis of the *Spitzer* observations of NGC 2264 leads us to conclude that we are identifying the primordial substructure of this cluster. Bright 24 μm sources, spatially arranged in unusual linear patterns, were found to be lying along and within dense fingers of molecular material with a spacing similar to that expected for simple Jeans fragmentation. These sources are likely very young if we consider the short crossing times of the associated sub-millimeter and millimeter cores suggested by Williams & Garland (2002) of 0.5 Myr and Peretto et al. (2005) of 0.63 Myr, respectively. In fact, we find the majority ($\sim 60\%$) of these sources to be Class I sources and protostellar candidates, suggesting that star formation in the Spokes cluster is occurring primarily within dense filamentary molecular structures.

Primordial filamentary substructuring of this kind has also been found in the Trapezium cluster, in Orion. Lada et al. (2004), by analyzing deep ground-based 3.4 μm observations of the Trapezium, find a deeply embedded population of young objects that traces a filamentary molecular ridge lying behind the main cluster. The older, more evolved foreground population in the Trapezium is distributed in a more dispersed manner with an

isothermal-like distribution. Similar to the Trapezium, NGC 2264 also exhibits a somewhat older and more dispersed population near the Spokes cluster (Lada & Lada 2003). Williams & Garland (2002) observed H^{13}CO^+ emission lines and Peretto et al. (2005) observed N_2H^+ lines toward the sub-millimeter and millimeter peaks in the Spokes cluster, which they used to measure the core velocity dispersion and infer the virial mass of the system. They find that the virial mass is less than the total gas and dust mass enveloping the cluster. This means that the cores within the dusty filaments are currently bound to the filaments. If the total stellar mass of the cluster is less than the total mass of the dense gas in the filaments then the stellar group is destined to become unbound if the surrounding gas and dust is rapidly dispersed. This situation suggests that after star formation occurs in filamentary molecular fragments of the cloud, the more recently formed stars eventually expand to merge with the older population as the cloud material is rapidly cleared through outflows and jets, leading to the less structured distributions of the overall population (Bonnell et al. 2003).

Finally, we find that the bright 24 μm sources appear to have a preferential separation between themselves of $20'' \pm 5''$. This distance is in very good agreement with the Jeans length corresponding to the mean density of the IRS-2 region determined by Williams & Garland (2002). It appears we are observing the result of the thermal fragmentation of the dense filamentary material into quasi-equidistant star-forming cores. On the other hand, turbulent motions appear to be present in this region: Peretto et al. (2005) find that the millimeter peaks have velocity dispersions greater than the thermal sound speed for molecular gas at 15 K. Perhaps the dusty filaments may have formed through turbulent motions of the cloud (Bonnell et al. 2003), then as the turbulence decayed the filaments became thermalized and fragmented into star-forming cores. The newly formed stars would generate outflows that re-energize the surrounding region, feeding turbulence back into the cores and filaments and eventually disrupting the cloud. The positions of the young protostars may be the only remaining indication that thermal pressure played an important role in the formation of these objects.

We are indebted to Grace Wolf-Chase for kindly sharing with us her sub-millimeter data. PT acknowledges support from the scholarship SFRH/BD/13984/2003 awarded by the Fundação para a Ciência e Tecnologia (Portugal). This work is based on observations made with the *Spitzer* Space Telescope, which is operated by the Jet Propulsion Laboratory, California Institute of Technology under NASA contracts 1407 and 960785.

REFERENCES

- Bertin, E., & Arnouts, S. 1996, *A&AS*, 117, 393
 Bonnell, I. A., Bate, M. R., & Vine, S. G. 2003, *MNRAS*, 343, 413
 Castelain, M. W., & Grasdalen, G. 1988, *ApJ*, 335, 150
 Dahm, S. E. & Simon, T. 2005, *AJ*, 129, 829
 Elmegreen, B. G., Efremov, Y., Pudritz, R. E., & Zinnecker, H. 2000, *Protostars and Planets IV*, 179
 Fazio, G. G., et al. 2004, *ApJS*, 154, 10
 Gordon, K. et al. 2005, *PASP*, 117, 503.
 Hartmann, L. 2002, *ApJ*, 578, 914
 Herbig, G. H. 1954, *ApJ*, 119, 483
 Li, A., & Draine, B. T. 2002, *ApJ*, 572, 232
 Lada, C. J. 1987, *IAU Symp.* 115: Star Forming Regions, 115, 1
 Lada, C. J., & Lada, E. A. 2003, *ARA&A*, 41, 57
 Lada, C. J., Muench, A. A., Lada, E. A., & Alves, J. F. 2004, *AJ*, 128, 1254

- Lada, C. J., Muench, A. A., Luhman, K. L., Allen, L., Hartman, L., Megeath, T., Myers, P., Fazio, G., Wood, K., Muzerolle, J., Rieke, G., Siegler, N. & Young, E. 2005, ApJ, submitted
- Margulis, M., Lada, C. J., & Snell, R. L. 1988, ApJ, 333, 316
- Margulis, M., Lada, C. J., & Young, E. T. 1989, ApJ, 345, 906
- Peretto, N., André, P., Belloche, A. 2005, A&A, in press
- Reipurth, B., Yu, K., Moriarty-Schieven, G., Bally, J., Aspin, C., & Heathcote, S. 2004, AJ, 127, 1069
- Rieke, G.H., et al. 2004, ApJS, 154, 25.
- Sargent, A. I., van Duinen, R. J., Nordh, H. L., Fridlund, C. V. M., Aalders, J. W., & Beintema, D. 1984, A&A, 135, 377
- Schwartz, P. R., Thronson, H. A., Odenwald, S. F., Glaccum, W., Loewenstein, R. F., & Wolf, G. 1985, ApJ, 292, 231
- Simon, T., & Dahm, S. E. 2005, ApJ, 618, 795
- Walker, M. F. 1954, AJ, 59, 333
- Ward-Thompson, D., Zylka, R., Mezger, P. G., & Sievers, A. W. 2000, A&A, 355, 1122
- Williams, J. P., & Garland, C. A. 2002, ApJ, 568, 259
- Wolf-Chase, G., Moriarty-Schieven, G., Fich, M., & Barsony, M. 2003, MNRAS, 344, 809